

The Spin-orbit force, recoil corrections and possible $B\bar{B}^*$ and $D\bar{D}^*$ molecular states

Lu Zhao^{1*}, Li Ma^{1†}, Shi-Lin Zhu^{1,2‡}

¹ *Department of Physics and State Key Laboratory of Nuclear Physics and Technology, Peking University, Beijing 100871, China*

² *Collaborative Innovation Center of Quantum Matter, Beijing 100871, China*

In the framework of the one boson exchange model, we have calculated the effective potentials between two heavy mesons $B\bar{B}^*$ and $D\bar{D}^*$ from the t- and u-channel π , η , ρ , ω and σ meson exchange with four kinds of quantum number: $I = 0, J^{PC} = 1^{++}$; $I = 0, J^{PC} = 1^{+-}$; $I = 1, J^{PC} = 1^{++}$; $I = 1, J^{PC} = 1^{+-}$. We keep the recoil corrections to the $B\bar{B}^*$ and $D\bar{D}^*$ system up to $O(\frac{1}{M^2})$. The spin orbit force appears at $O(\frac{1}{M})$, which turns out to be important for the very loosely bound molecular states. Our numerical results show that the momentum-related corrections are unfavorable to the formation of the molecular states in the $I = 0, J^{PC} = 1^{++}$ and $I = 1, J^{PC} = 1^{+-}$ channels in the $D\bar{D}^*$ systems.

PACS numbers: 13.75.-n, 13.75.Cs, 14.20.Gk

I. INTRODUCTION

The charmonium spectroscopy has been studied extensively during the last few years. The states below the open charm threshold are all observed now while many states above the open charm threshold are still missing. On the other hand, a large number of charmonium-like states (or so called XYZ states) have been observed by experimental collaborations such as Belle, Barbar, CDF, D0, LHCb, BESIII, CLEOC. These XYZ states decay into the conventional charmonium, but some of them do not fit into the quark model charmonium spectrum easily. Especially the charged charmonium-like signals are the good candidates of the exotic states, such as $Z(4430)$ observed in the $\psi'\pi^\pm$ modes, $Z_1(4050)$, $Z_2(4250)$ in the $\chi_{c1}\pi^\pm$ modes in the B meson decays [1–3], $Z_c(4025)^\pm$ in the π^\pm recoil mass spectrum and $Z_c(4020)^\pm$ in the $\pi^\pm h_c$ mass spectrum [4]. Recently, the BES Collaboration announced a charged structure $Z_c(3900)$ in the $\pi^\pm J/\psi$ invariant mass spectrum of the process $e^+e^- \rightarrow \pi^\pm J/\psi$ at a center-of-mass (CM) energy of $\sqrt{s} = 4.260 \pm 0.001 \text{ GeV}$ [4]. How to explain the underlying structure of these charmonium-like states becomes an important issue.

Many theoretical schemes were proposed to explain these XYZ states, including the molecular states [5–10], hybrid charmonium [11], tetraquark states [12–17], dynamically generated resonances [18]. Among the above schemes, the molecular picture provides a plausible explanation since some XYZ states are very close to the thresholds of a pair of charmed meson.

Since the first observation of $X(3872)$ by the Belle Collaboration [19] in the exclusive decay process $B^\pm \rightarrow K^\pm \pi^+ \pi^- J/\psi$, its interpretation as a molecular candidate of the $D\bar{D}^*$ system has been investigated by many theoretical groups [7, 8][20–27]. Due to the same intriguing near-threshold nature, the recently observed two charged bottomonium-like states $Z_b(10610)$ and $Z_b(10650)$ by the Belle observation [28] were also interpreted as good candidates of the $B\bar{B}^*$ and $B^*\bar{B}^*$

molecular states [29–33]. The newly observed $Z_c(3900)$ by BESIII collaborations [4], CLEOC [34] and Belle with ISR [35] is also close to the threshold of $D\bar{D}^*$. In many references, it was interpreted as the isovector partner of the well established isoscalar state $X(3872)$ with the same quantum number $J^P = 1^+$ [42–44].

When investigating the possibility of $X(3872)$ as the $D\bar{D}^*$ molecular state with $J^{PC} = 1^{++}$, the one-pion-exchange (OPE) model and one-boson-exchange (OBE) model were used to calculate the binding energy of the $D\bar{D}^*$ system in the Ref.[36]. In Ref.[33], the OBE model was applied to investigate the possibility of $Z_b(10610)$ and $Z_b(10650)$ as the molecular states of the $B\bar{B}^*$ and $B^*\bar{B}^*$ system.

With the exchange of the light pseudoscalar, vector and scalar mesons, the OBE model provides an effective framework to describe the interaction between two hadrons at different range. In the previous work, the heavy quark symmetry is always invoked to simplify the calculation in the derivation of the interaction potential between two heavy mesons such as $D\bar{D}^*$ or $B\bar{B}^*$. Moreover, the three momentum of the external particles is sometimes ignored. Hence the resulting potential between the heavy mesons depends on the exchanged momentum only. All the recoils corrections were omitted.

The possible $D\bar{D}^*$ or $B\bar{B}^*$ molecular system is very close to the two heavy meson threshold. The binding energy is sometime quite small. Especially in the case of $X(3872)$, its binding energy may be less than 1 MeV if it turns out to be a $D\bar{D}^*$ molecule. Compared to the tiny binding energy, the higher order recoil corrections may turn out to be non-negligible.

In the present work, we keep the momentum of the initial and final states explicitly and derive the effective potential using the relativistic Lagrangian. We will keep the recoil corrections up to the order $\frac{1}{M^2}$, where M is the mass of the component in the system. Especially the spin-orbit force first appears at $O(\frac{1}{M})$. With the effective potentials with the explicit recoil corrections $O(\frac{1}{M^2})$, we carefully investigate the $D\bar{D}^*$ system with $I = 0, J^{PC} = 1^{++}$ to measure the $\frac{1}{M^2}$ correction for $X(3872)$, $D\bar{D}^*$ system with $I = 1, J^{PC} = 1^+$ for $Z_c(3900)$, and $B\bar{B}^*$ with $I = 1, J^{PC} = 1^+$ for $Z_b(10610)$. Numerically, these recoil corrections are quite important in the loosely bound heavy meson systems. Especially, the recoil correction is comparable to the binding energy in the case of

*Email: Luzhao@pku.edu.cn

†Email: lima@pku.edu.cn

‡Email: zhushl@pku.edu.cn

X(3872).

This paper is organized as follows. We first introduce the formalism of the derivation of the effective potential in Section II. We present our numerical results in Section III. The last section is the summary and discussion. We collect some lengthy formulae in the appendix.

II. THE EFFECTIVE POTENTIAL

A. Wave function, Effective Lagrangian and Coupling constants

First, we construct the flavor wave functions of the isovector and isoscalar molecular states composed of the $B\bar{B}^*$ and $D\bar{D}^*$ as in Refs. [29, 30]. The flavor wave function of the $B\bar{B}^*$ system reads

$$\begin{cases} |1, 1\rangle = \frac{1}{\sqrt{2}}(|B^{*+}\bar{B}^0\rangle + c|B^+\bar{B}^{*0}\rangle), \\ |1, -1\rangle = \frac{1}{\sqrt{2}}(|B^{*-}\bar{B}^0\rangle + c|B^-\bar{B}^{*0}\rangle), \\ |1, 0\rangle = \frac{1}{2}[(|B^{*+}B^- \rangle - |B^{*0}\bar{B}^0\rangle) + c(|B^+B^{*-}\rangle - |B^0\bar{B}^{*0}\rangle)], \end{cases} \quad (1)$$

$$|0, 0\rangle = \frac{1}{2}[(|B^{*+}B^- \rangle + |B^{*0}\bar{B}^0\rangle) + c(|B^+B^{*-}\rangle + |B^0\bar{B}^{*0}\rangle)] \quad (2)$$

where $c = \pm$ corresponds to C-parity $C = \mp$ respectively. For the $D\bar{D}^*$ system

$$\begin{cases} |1, 1\rangle = \frac{1}{\sqrt{2}}(|\bar{D}^{*0}D^+\rangle + c|\bar{D}^0D^{*+}\rangle), \\ |1, -1\rangle = \frac{1}{\sqrt{2}}(|\bar{D}^{*0}D^-\rangle + c|\bar{D}^0D^{*-}\rangle), \\ |1, 0\rangle = \frac{1}{2}[(|\bar{D}^{*0}D^0\rangle - |\bar{D}^{*-}D^+\rangle) + c(|\bar{D}^0D^{*0}\rangle - |\bar{D}^-D^{*+}\rangle)], \end{cases} \quad (3)$$

$$|0, 0\rangle = \frac{1}{2}[(|\bar{D}^{*0}D^0\rangle + |\bar{D}^{*-}D^+\rangle) + c(|\bar{D}^0D^{*0}\rangle + |\bar{D}^-D^{*+}\rangle)] \quad (4)$$

Since the C-parity of $Z_b(10610)^0$ is odd, we will take the coefficient $c = +$ for the $B\bar{B}^*$ system. While the C parity of X(3872) was even, the $I = 0$ $D\bar{D}^*$ system will take the coefficient $c = -$. Moreover, we will consider both two C-parity option for the $I = 1$ $D\bar{D}^*$ system.

The meson exchange Feynman diagrams for both the $B\bar{B}^*$ and $D\bar{D}^*$ systems at the tree level are shown in Fig. 1 and Fig. 2.

Based on the chiral symmetry, the Lagrangian for the pseudoscalar, scalar and vector meson interaction with the heavy flavor mesons reads

$$\begin{aligned} \mathcal{L}_P = & -i\frac{2g}{f_\pi}\bar{M}P_b^{*\mu}\partial_\mu\phi_{ba}P_a^\dagger + i\frac{2g}{f_\pi}\bar{M}P_b\partial_\mu\phi_{ba}P_a^{*\mu\dagger} \\ & - \frac{g}{f_\pi}P_b^{*\mu}\partial^\alpha\phi_{ba}\partial^\beta P_a^{*\nu\dagger}\epsilon_{\mu\nu\alpha\beta} + \frac{g}{f_\pi}\partial^\beta P_b^{*\mu}\partial^\alpha\phi_{ba}P_a^{*\nu\dagger}\epsilon_{\mu\nu\alpha\beta} \end{aligned} \quad (5)$$

$$\begin{aligned} \widetilde{\mathcal{L}}_P = & -i\frac{2g}{f_\pi}\widetilde{M}P_a^{*\mu}\partial_\mu\phi_{ab}\widetilde{P}_b^{*\mu} - i\frac{2g}{f_\pi}\widetilde{M}P_a^{*\mu\dagger}\partial_\mu\phi_{ab}\widetilde{P}_b \\ & + \frac{g}{f_\pi}\partial^\beta P_a^{*\mu\dagger}\partial^\alpha\phi_{ab}\widetilde{P}_b^{*\nu}\epsilon_{\mu\nu\alpha\beta} - \frac{g}{f_\pi}\widetilde{P}_a^{*\mu\dagger}\partial^\alpha\phi_{ab}\partial^\beta\widetilde{P}_b^{*\nu}\epsilon_{\mu\nu\alpha\beta} \end{aligned} \quad (6)$$

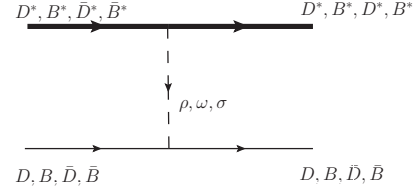


FIG. 1: The direct-channel Feynman diagrams for both the $D\bar{D}^*$ and $B\bar{B}^*$ systems at the tree level. The thick line represents the vector state D^*, B^*, \bar{D}^* or \bar{B}^* while the thin line stands for D, B, \bar{D} and \bar{B} .

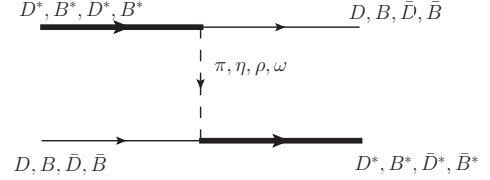


FIG. 2: The cross-channel Feynman diagrams for both the $D\bar{D}^*$ and $B\bar{B}^*$ systems at the tree level. Notations are the same as in Fig. 1

$$\begin{aligned} \mathcal{L}_V = & i\frac{\beta g_v}{\sqrt{2}}P_bV_{ba}^\mu\partial_\mu P_a^\dagger - i\frac{\beta g_v}{\sqrt{2}}\partial_\mu P_bV_{ba}^\mu P_a^\dagger \\ & - i\sqrt{2}\lambda g_v\epsilon_{\mu\alpha\beta\nu}\partial^\mu P_b\partial^\alpha V_{ba}^\beta P_a^{*\nu\dagger} \\ & - i\sqrt{2}\lambda g_v\epsilon_{\mu\alpha\beta\nu}P_b^{*\mu}\partial^\alpha V_{ba}^\beta\partial^\nu P_a^\dagger \\ & - i\frac{\beta g_v}{\sqrt{2}}P_b^{*\nu}V_{ba}^\mu\partial_\mu P_{va}^\dagger + i\frac{\beta g_v}{\sqrt{2}}\partial_\mu P_b^{*\nu}V_{ba}^\mu P_{va}^{*\dagger} \\ & - i2\sqrt{2}\lambda g_v\bar{M}^*P_b^{*\mu}(\partial_\mu V_\nu - \partial_\nu V_\mu)_{ba}P_a^{*\nu\dagger}, \end{aligned} \quad (7)$$

$$\begin{aligned} \widetilde{\mathcal{L}}_V = & -i\frac{\beta g_v}{\sqrt{2}}\partial_\mu\widetilde{P}_a^\dagger V_{ab}^\mu\widetilde{P}_b + i\frac{\beta g_v}{\sqrt{2}}\widetilde{P}_a^\dagger V_{ab}^\mu\partial_\mu\widetilde{P}_b \\ & + i\sqrt{2}\lambda g_v\epsilon_{\mu\alpha\beta\nu}\widetilde{P}_a^{*\mu\dagger}\partial^\alpha V_{ab}^\beta\partial^\nu\widetilde{P}_b \\ & + i\sqrt{2}\lambda g_v\epsilon_{\mu\alpha\beta\nu}\partial^\mu\widetilde{P}_a^\dagger\partial^\alpha V_{ab}^\beta\widetilde{P}_b^{*\nu} \\ & + i\frac{\beta g_v}{\sqrt{2}}\partial_\mu\widetilde{P}_{va}^{*\dagger}V_{ba}^\mu\widetilde{P}_b^{*\nu} - i\frac{\beta g_v}{\sqrt{2}}\widetilde{P}_{va}^{*\dagger}V_{ab}^\mu\partial_\mu\widetilde{P}_b^{*\nu} \\ & - i2\sqrt{2}\lambda g_v\bar{M}^*\widetilde{P}_a^{*\mu\dagger}(\partial_\mu V_\nu - \partial_\nu V_\mu)_{ab}\widetilde{P}_b^{*\nu}, \end{aligned} \quad (8)$$

$$\mathcal{L}_S = -2g_s\bar{M}P_b\sigma P_b^\dagger + 2g_s\bar{M}^*P_b^{*\mu}\sigma P_{\mu b}^{*\dagger} \quad (9)$$

$$\widetilde{\mathcal{L}}_S = -2g_s\bar{M}\widetilde{P}_a^\dagger\sigma\widetilde{P}_a + 2g_s\bar{M}^*\widetilde{P}_{\mu a}^{*\dagger}\sigma\widetilde{P}_a^{*\mu} \quad (10)$$

where the heavy flavor meson fields P and P^* represent $P = (D^0, D^+)$ or (B^-, \bar{B}^0) and $P^* = (D^{*0}, D^{*+})$ or (B^{*-}, \bar{B}^{*0}) . Its

corresponding heavy anti-meson fields \tilde{P} and \tilde{P}^* represent $\tilde{P} = (\bar{D}^0, D^-)$ or (B^+, B^0) and $\tilde{P}^* = (\bar{D}^{*0}, D^{*-})$ or (B^{*+}, B^{*0}) . ϕ , V represent the the exchanged pseudoscalar and vector meson matrices, σ is the only scalar meson interacting with the heavy flavor meson.

$$\phi = \begin{pmatrix} \frac{\pi^0}{\sqrt{2}} + \frac{\eta}{\sqrt{6}} & \pi^+ \\ \pi^- & -\frac{\pi^0}{\sqrt{2}} + \frac{\eta}{\sqrt{6}} \end{pmatrix} \quad (11)$$

$$V = \begin{pmatrix} \frac{\rho^0}{\sqrt{2}} + \frac{\omega}{\sqrt{2}} & \rho^+ \\ \rho^- & -\frac{\rho^0}{\sqrt{2}} + \frac{\omega}{\sqrt{2}} \end{pmatrix} \quad (12)$$

According the OBE model, five mesons (π , σ , ρ , ω and η) contribute to the effective potential. In the $D\bar{D}^*$ and $B\bar{B}^*$ systems we considered, the potentials are the same for the three isovector states in Eqs. (1)~(4) with the exact isospin symmetry. Expanding the Lagrangian densities in Eqs. (5)~(10) leads to each meson's contribution for the two coupled channels. These channel-dependent coefficients are listed in Table II. The pionic coupling constant $g = 0.59$ is extracted from the width of D^{*+} [37]. $f_\pi = 132 \text{ MeV}$ is the pion decay constant. According the vector meson dominance mechanism, the parameters g_v and β can be determined as $g_v = 5.8$ and $\beta = 0.9$. At the same time, by matching the form factor obtained from the light cone sum rule and that calculated from the lattice QCD, we can get $\lambda = 0.56 \text{ GeV}^{-1}$ [38, 39]. The coupling constant related to the scalar meson exchange is $g_s = g_\pi/2\sqrt{6}$ with $g_\pi = 3.73$ [30, 40]. All these parameters are listed in Table I.

TABLE I: The coupling constants and masses of the heavy mesons and the exchanged light mesons used in our calculation. The masses of the mesons are taken from the PDG [41]

	mass(MeV)	coupling constants
pseudoscalar	$m_\pi = 134.98$	$g = 0.59$
	$m_\eta = 547.85$	$f_\pi = 132 \text{ MeV}$
vector	$m_\rho = 775.49$	$g_v = 5.8$
	$m_\omega = 782.65$	$\beta = 0.9$
		$\lambda = 0.56 \text{ GeV}^{-1}$
scalar	$m_\sigma = 600$	$g_s = g_\pi/2\sqrt{6}$
		$g_\pi = 3.73$
heavy flavor	$m_D = 1864.9$	
	$m_{D^*} = 2010.0$	
	$m_B = 5279.0$	
	$m_{B^*} = 5325$	

In order to include all the momentum-related terms in our calculation, we need introduce the polarization vectors of the vector mesons. The polarization vector at its rest frame is

$$\epsilon_\lambda = (0, \vec{\epsilon}_\lambda) \quad (13)$$

We need to make a lorentz boost to Eq. 13 to derive the polar-

TABLE II: coefficients

	isospin	direct-channel			cross-channel			
		ρ	ω	σ	ρ	ω	π	η
$D\bar{D}^*$	$I = 1$	-1/2	1/2	1	-c/2	c/2	-c/2	c/6
	$I = 0$	3/2	1/2	1	3c/2	c/2	3c/2	c/6
$B\bar{B}^*$	$I = 1$	-1/2	1/2	1	-c/2	c/2	-c/2	c/6
	$I = 0$	3/2	1/2	1	3c/2	c/2	3c/2	c/6

ization vector in the laboratory frame

$$\epsilon_\lambda^{lab} = (\frac{\vec{p} \cdot \vec{\epsilon}_\lambda}{m}, \vec{\epsilon}_\lambda + \frac{\vec{p} \cdot (\vec{p} \cdot \vec{\epsilon}_\lambda)}{m(P_0 + m)}) \quad (14)$$

where $p = (p_0, \mathbf{p})$ is the particle's 4-momentum in the laboratory frame and m is the mass of the particle.

B. Effective potential

Together with the wave function and Feynman diagram, we can derive the relativistic scattering amplitude at the tree level

$$\langle f|S|i\rangle = \delta_{fi} + i\langle f|T|i\rangle = \delta_{fi} + (2\pi)^4 \delta^4(p_f - p_i) iM_{fi}, \quad (15)$$

where the T-matrix is the interaction part of the S-matrix and M is defined as the invariant matrix element. After applying Bonn approximation on the Lippmann-Schwinger equation, the S-matrix reads

$$\langle f|S|i\rangle = \delta_{fi} - 2\pi\delta(E_f - E_i) iV_{fi} \quad (16)$$

with V_{fi} being the effective potential. Considering the different normalization conventions used for the scattering amplitude M_{fi} , T-matrix T_{fi} and V_{fi} , we have

$$V_{fi} = -\frac{M_{fi}}{\sqrt{\prod_f 2p_f^0 \prod_i 2p_i^0}} \approx -\frac{M_{fi}}{\sqrt{\prod_f 2m_f^0 \prod_i 2m_i^0}} \quad (17)$$

where $p_{f(i)}$ denotes the four momentum of the final (initial) state.

During our calculation, $P_1(E_1, \vec{p})$ and $P_2(E_2, -\vec{p})$ denote the four momenta of the initial particles in the center mass system, while $P_3(E_3, \vec{p}')$ and $P_4(E_4, -\vec{p}')$ denote the four momenta of the final particles, respectively.

$$q = P_3 - P_1 = (E_3 - E_1, \vec{p}' - \vec{p}) = (E_2 - E_4, \vec{q}) \quad (18)$$

is the transferred four momentum or the four momentum of the meson propagator. For convenience, we always use

$$\vec{q} = \vec{p}' - \vec{p} \quad (19)$$

and

$$\vec{k} = \frac{1}{2}(\vec{p}' + \vec{p}) \quad (20)$$

instead of \vec{p}' and \vec{p} in the practical calculation.

In the OBE model, each vertex in the Feynman diagram needs a form factor to suppress the high momentum contribution. We take the conventional form for the form factor as in the Bonn potential model.

$$F(q) = \frac{\Lambda^2 - m_\alpha^2}{\Lambda^2 - q^2} = \frac{\Lambda^2 - m_\alpha^2}{\tilde{\Lambda}^2 + \vec{q}^2} \quad (21)$$

m_α is the mass of the exchanged meson and

$$\tilde{\Lambda}^2 = \Lambda^2 - (m^* - m)^2 \quad (22)$$

where m and m^* is the mass of the heavy flavor meson D and D^* or B and B^* . So far, the effective potential is in the momentum space. In order to solve the time independent Schrödinger equation in the coordinate space, we need to make the Fourier transformation to $V(\vec{q}, \vec{k})$. The details of the Fourier transformations are presented in the Appendix.

All the meson exchanged potentials for $B\bar{B}^*$ and $D\bar{D}^*$ are the same, except the π exchange potential. The π mass is larger than the mass difference of B and \bar{B}^* but smaller than that of D and \bar{D}^* .

The expressions of the direct-channel effective potential through exchanging the σ , ρ mesons are

$$\begin{aligned} V_\sigma = & -C_\sigma g_s^2 (\vec{\epsilon}_b \cdot \vec{\epsilon}_a^\dagger) F_{1t\sigma} \\ & -C_\sigma g_s^2 \frac{1}{2m^{*2}} (F_{3t1\sigma} + F_{3t2\sigma}) \\ & +C_\sigma g_s^2 \frac{1}{2m^{*2}} \frac{(\vec{\epsilon}_b \times \vec{\epsilon}_a^\dagger) \cdot \vec{L}}{i} F_{5t\sigma} \end{aligned} \quad (23)$$

$$\begin{aligned} V_\rho = & -C_\rho \beta^2 g_v^2 \frac{\vec{\epsilon}_b \cdot \vec{\epsilon}_a^\dagger}{2} F_{1t\rho} \\ & +C_\rho \left(\frac{\lambda \beta g_v^2}{m^*} - \frac{\beta^2 g_v^2}{4m^{*2}} \right) (F_{3t1\rho} + F_{3t2\rho}) \\ & -C_\rho \beta^2 g_v^2 \frac{\vec{\epsilon}_b \cdot \vec{\epsilon}_a^\dagger}{2mm^*} [F_{4t1\rho} + \{-\frac{1}{2}\nabla^2, F_{4t2\rho}\}] \\ & +C_\rho \left(\frac{\beta^2 g_v^2}{4m^{*2}} - \lambda \beta g_v^2 \frac{m^* + m}{mm^*} \right) \frac{(\vec{\epsilon}_b \times \vec{\epsilon}_a^\dagger) \cdot \vec{L}}{i} F_{5t\rho} \end{aligned} \quad (24)$$

The ω and ρ meson exchange potentials have the same form except that the meson mass and channel-dependent coefficients are different.

The expression of the cross-channel effective potential through exchanging the π meson in the $B\bar{B}^*$ system is

$$\begin{aligned} V_\pi = & CC_\pi \frac{g_\pi^2 (m^* + m)^2}{f_\pi^2 4m^{*2}} (F_{3u1\pi} + F_{3u2\pi}) \\ & +CC_\pi \frac{g_\pi^2 m^{*2} - m^2}{f_\pi^2 2m^{*2}} \frac{(\vec{\epsilon}_b \times \vec{\epsilon}_a^\dagger) \cdot \vec{L}}{i} F_{5u\pi} \\ & -CC_\pi \frac{g_\pi^2 (m^* - m)^2}{f_\pi^2 m^{*2}} (F_{6u1} + F_{6u2\pi} \nabla + F_{6u3\pi} \nabla^2) \end{aligned} \quad (25)$$

The expression of the cross-channel effective potential

through exchanging the π meson in the $D\bar{D}^*$ system is

$$\begin{aligned} V'_\pi = & CC_\pi \frac{g_\pi^2 (m^* + m)^2}{f_\pi^2 4m^{*2}} (F'_{3u1\pi} + F'_{3u2\pi}) \\ & +CC_\pi \frac{g_\pi^2 m^{*2} - m^2}{f_\pi^2 2m^{*2}} \frac{(\vec{\epsilon}_b \times \vec{\epsilon}_a^\dagger) \cdot \vec{L}}{i} F'_{5u\pi} \\ & -CC_\pi \frac{g_\pi^2 (m^* - m)^2}{f_\pi^2 m^{*2}} (F'_{6u1} + F'_{6u2\pi} \nabla + F'_{6u3\pi} \nabla^2) \end{aligned} \quad (26)$$

The expression of the cross-channel effective potential through exchanging the ρ meson is

$$\begin{aligned} V_\rho = & -CC_\rho \lambda^2 g_v^2 \frac{(m^* + m)^2}{2mm^*} (\vec{\epsilon}_b \cdot \vec{\epsilon}_a^\dagger) F_{2u\rho} \\ & +CC_\rho \lambda^2 g_v^2 \frac{(2m^* - m)(m^* + m)^2}{2m^{*3}} (F_{3u1\rho} + F_{3u2\rho}) \\ & +CC_\rho \lambda^2 g_v^2 \frac{2(m^* - m)^2}{mm^*} \vec{\epsilon}_b \cdot \vec{\epsilon}_a^\dagger [F_{4u1\rho} + \{-\frac{1}{2}\nabla^2, F_{4u2\rho}\}] \\ & -CC_\rho \lambda^2 g_v^2 \frac{m(m^{*2} - m^2)}{m^{*3}} \frac{(\vec{\epsilon}_b \times \vec{\epsilon}_a^\dagger) \cdot \vec{L}}{i} F_{5u\rho} \\ & +CC_\rho \lambda^2 g_v^2 \frac{2(2m^* + m)(m^* - m)^2}{m^{*3}} (F_{6u1\rho} + F_{6u2\rho} \nabla \\ & + F_{6u3\rho} \nabla^2) \end{aligned} \quad (27)$$

Similarly, the η and π meson exchange potential has the same form in the $B\bar{B}^*$ system. The potential from the ω and ρ meson exchange is also similar except the meson mass and channel-dependent coefficients. The explicit forms of $\mathcal{F}_{\mu\alpha}, \mathcal{F}_{\mu\alpha}, \mathcal{F}_{\mu\nu\alpha}, \mathcal{F}'_{\mu\alpha}, \mathcal{F}'_{\mu\alpha}, \mathcal{F}'_{\mu\nu\alpha}$ are shown in the Appendix.

In our calculation, we explicitly consider the external momentum of the initial and final states. Due to the recoil corrections, several new terms appear which were omitted in the heavy quark symmetry limit. These momentum dependent terms are related to the momentum $\vec{k} = \frac{1}{2}(\vec{p}' + \vec{p})$:

$$\frac{\vec{k}^2}{\vec{q}^2 + m_\alpha^2} \quad (28)$$

and

$$\frac{i\vec{S} \cdot \vec{k} \times \vec{q}}{\vec{q}^2 + m_\alpha^2} \quad (29)$$

and

$$\frac{(\vec{\epsilon}_b \cdot \vec{k})(\vec{\epsilon}_a^\dagger \cdot \vec{k})}{\vec{p}^2 + m_\alpha^2} \quad (30)$$

where $\vec{S} = -i(\vec{\epsilon}_b \times \vec{\epsilon}_a^\dagger)$. The term in Eq. (29) is the well-known spin orbit force. The term in Eq. (30) depends on the spin and results in the momentum-related operator ∇, ∇^2 . The Fourier transformation of the above new interaction terms are also shown in the Appendix. In short, all the terms in the effective potentials in the form of $F_{4t1\rho}, F'_{5u\pi}, (F_{6u1\rho} + F_{6u2\rho} \nabla + F_{6u3\rho} \nabla^2)$ etc with the sub-indices 4, 5, 6 arise from the recoil corrections and vanish when the heavy meson mass m, m^* goes to infinity. Especially, the spin orbit force appears at $O(1/M)$!

C. Schrödinger equation

With the effective potential $V(\vec{r})$ in Eqs. (23) ~ (27), we are able to study the binding property of the system by solving the Schrödinger Equation

$$\left(-\frac{\hbar^2}{2\mu}\nabla^2 + V(\vec{r}) - E\right)\Psi(\vec{r}) = 0, \quad (31)$$

where $\Psi(\vec{r})$ is the total wave function of the system. The total spin of the system $S = 1$ and the orbital angular momenta $L = 0$ and $L = 2$. Thus the wave function $\Psi(\vec{r})$ should have the following form

$$\Psi(\vec{r}) = \psi_S(\vec{r}) + \psi_D(\vec{r}), \quad (32)$$

where $\psi_S(\vec{r})$ and $\psi_D(\vec{r})$ are the S -wave and D -wave functions, respectively. In the matrix method, we use Laguerre polynomials as a set of orthogonal basis

$$\chi_{nl}(r) = \sqrt{\frac{(2l)(2l+3)n!}{\Gamma(2l+3+n)}} r^l e^{-\lambda r} L_n^{2l+2}(2\lambda r), n = 1, 2, 3... \quad (33)$$

with a normalization condition of

$$\int_0^\infty \chi_{im}(r)\chi_{in}(r)r^2 dr = \delta_{ij}\delta_{mn}. \quad (34)$$

We expand the total wave function as

$$\Psi(\vec{r}) = \sum_{i=0}^{n-1} a_i \chi_{i0}(r) \phi_S + \sum_{p=0}^{n-1} b_p \chi_{p2}(r) \phi_D, \quad (35)$$

where ϕ_S and ϕ_D are the angular part of the spin and orbital wave function for the S - and D -states, respectively. a_i and b_i are the corresponding expansion coefficients.

In the practical calculation, we detach the terms related to the kinetic-energy-operator ∇^2 and ∇ from $V(\vec{r})$ and re-write Eq. (31) as

$$\left(-\frac{\hbar^2}{2\mu}\nabla^2 - \frac{\hbar^2}{2\mu}[\nabla^2\alpha(r) + \alpha(r)\nabla^2] + \alpha_1(r)\nabla + \alpha_2(r)\nabla^2 + \tilde{V}(\vec{r}) - E\right)\Psi(\vec{r}) = 0 \quad (36)$$

with

$$\nabla^2 = \frac{1}{r} \frac{d^2}{dr^2} r - \frac{\vec{L}^2}{r^2}, \quad (37)$$

in which $\alpha(r), \alpha_1(r)$ and $\alpha_2(r)$ are

$$\begin{aligned} \alpha(r) = & (-2\mu)(-C_\rho \beta^2 g_v^2 \frac{\vec{\epsilon}_b \cdot \vec{\epsilon}_a^\dagger}{2mm^*} \mathcal{F}_{4i2\rho} - C_\omega \beta^2 g_v^2 \frac{\vec{\epsilon}_b \cdot \vec{\epsilon}_a^\dagger}{2mm^*} \mathcal{F}_{4i2\omega} \\ & + CC_\rho \lambda^2 g_v^2 \frac{2(m^* - m)^2}{mm^*} \vec{\epsilon}_b \cdot \vec{\epsilon}_a^\dagger F_{4u2\rho} \\ & + CC_\omega \lambda^2 g_v^2 \frac{2(m^* - m)^2}{mm^*} \vec{\epsilon}_b \cdot \vec{\epsilon}_a^\dagger F_{4u2\omega}) \end{aligned} \quad (38)$$

$$\begin{aligned} \alpha_1(r) = & CC_\pi \frac{g_\pi^2}{f_\pi^2} \frac{(m^* - m)^2}{m^{*2}} F'_{6u2\pi} \\ & + CC_\eta \frac{g_\eta^2}{f_\eta^2} \frac{(m^* - m)^2}{m^{*2}} F'_{6u2\eta} \\ & + CC_\rho \lambda^2 g_v^2 \frac{2(2m^* + m)(m^* - m)^2}{m^{*3}} F_{6u2\rho} \\ & + CC_\omega \lambda^2 g_v^2 \frac{2(2m^* + m)(m^* - m)^2}{m^{*3}} F_{6u2\omega} \end{aligned} \quad (39)$$

$$\begin{aligned} \alpha_2(r) = & C_\pi \frac{g_\pi^2}{f_\pi^2} \frac{(m^* - m)^2}{m^{*2}} F'_{6u3\pi} \\ & + CC_\eta \frac{g_\eta^2}{f_\eta^2} \frac{(m^* - m)^2}{m^{*2}} F_{6u3\eta} \\ & + CC_\rho \lambda^2 g_v^2 \frac{2(2m^* + m)(m^* - m)^2}{m^{*3}} F_{6u3\rho} \\ & + CC_\omega \lambda^2 g_v^2 \frac{2(2m^* + m)(m^* - m)^2}{m^{*3}} F_{6u3\omega} \end{aligned} \quad (40)$$

Then, with the wave function in Eq. (35), the Hamiltonian matrix can be expressed as

$$\begin{pmatrix} H^{SS} & H^{SD} \\ H^{DS} & H^{DD} \end{pmatrix} \quad (41)$$

with

$$\begin{aligned} H^{SS} = & \langle \phi_S | \int_0^\infty \sum_{i,j}^{n-1} a_i \chi_{i0}(r) \left\{ -\frac{\hbar^2}{2\mu} [1 + \alpha(r)] \nabla^2 a_j \chi_{j0}(r) \right. \\ & - \frac{\hbar^2}{2\mu} \nabla^2 [\alpha(r) a_j \chi_{j0}(r)] + \alpha_1(r) \nabla a_j \chi_{j0}(r) \\ & \left. + \alpha_2(r) \nabla^2 a_j \chi_{j0}(r) + V_{SS}(r) a_j \chi_{j0}(r) \right\} r^2 dr | \phi_S \rangle, \end{aligned} \quad (42)$$

$$H^{SD} = \langle \phi_S | \int_0^\infty \sum_{i,p}^{n-1} a_i \chi_{i0}(r) V_{SD}(r) b_p \chi_{p2}(r) r^2 dr | \phi_D \rangle, \quad (43)$$

$$H^{DS} = \langle \phi_D | \int_0^\infty \sum_{p,i}^{n-1} b_p \chi_{p2}(r) V_{DS}(r) a_i \chi_{i0}(r) r^2 dr | \phi_S \rangle, \quad (44)$$

and

$$\begin{aligned} H^{DD} = & \langle \phi_D | \int_0^\infty \sum_{p,q}^{n-1} b_p \chi_{p2}(r) \left\{ -\frac{\hbar^2}{2\mu} [1 + \alpha(r)] \nabla^2 b_q \chi_{q2}(r) \right. \\ & - \frac{\hbar^2}{2\mu} \nabla^2 [\alpha(r) b_q \chi_{q2}(r)] + \alpha_1(r) \nabla b_q \chi_{q2}(r) \\ & \left. + \alpha_2(r) \nabla^2 b_q \chi_{q2}(r) + V_{DD}(r) b_q \chi_{q2}(r) \right\} r^2 dr | \phi_D \rangle. \end{aligned} \quad (45)$$

The total Hamiltonian contains three angular momentum related operators $\hat{\vec{\epsilon}}_b \cdot \hat{\vec{\epsilon}}_a^\dagger, \hat{S}_{12}, (\hat{\vec{\epsilon}}_b \times \hat{\vec{\epsilon}}_a^\dagger) \cdot \hat{\vec{L}}$, which corresponds to

the spin-spin interaction, the spin orbit force and tensor force respectively. They act on the S and D-wave coupled wave functions and split the total effective potential $\tilde{V}(\vec{r})$ into the subpotentials $V_{SS}(r)$, $V_{SD}(r)$, $V_{DS}(r)$ and $V_{DD}(r)$. The matrix form reads

$$\langle \phi_S + \phi_D | \hat{\vec{e}}_b \cdot \hat{\vec{e}}_a \tilde{V}(\vec{r}) | \phi_S + \phi_D \rangle = \begin{pmatrix} V_{SS}(r) & 0 \\ 0 & V_{DD}(r) \end{pmatrix} \quad (46)$$

$$\langle \phi_S + \phi_D | \hat{S}_{12} \tilde{V}(\vec{r}) | \phi_S + \phi_D \rangle = \begin{pmatrix} 0 & -\sqrt{2}V_{SD}(r) \\ -\sqrt{2}V_{DS}(r) & 1 \end{pmatrix} \quad (47)$$

$$\langle \phi_S + \phi_D | (\hat{\vec{e}}_b \times \hat{\vec{e}}_a) \cdot \hat{\vec{L}} \tilde{V}(\vec{r}) | \phi_S + \phi_D \rangle = \begin{pmatrix} 0 & 0 \\ 0 & 3iV_{DD}(r) \end{pmatrix} \quad (48)$$

where the tensor force operator \hat{S}_{12} mixes the S-wave and D-wave contribution and is defined as

$$\hat{S}_{12} = 3(\vec{r} \cdot \hat{\vec{e}}_b)(\vec{r} \cdot \hat{\vec{e}}_a) - \hat{\vec{e}}_b \cdot \hat{\vec{e}}_a \quad (49)$$

III. NUMERICAL RESULTS

We diagonalize the Hamiltonian matrix to obtain the eigenvalue and eigenvector. If there exists a negative eigenvalue, there exists a bound state. The corresponding eigenvector is the wave function. We use the variation principle to solve the equation. We change the variable parameter to get the lowest eigenvalue. We also change the number of the basis functions to reach a stable result.

A. X(3872)

The mass of the π meson is smaller than the mass difference of D and \bar{D}^* , which causes the Fourier transformation of the π -meson-exchange potential to be a complex function. The different treatment of this complex potential would lead to quite different results for the system. In our approach, we drop the imaginary part of the potential.

In order to distinguish each meson's effect, we plot each meson's S-wave contribution to the potential in the first figure in Fig.4. The π meson provides the most attractive force while the σ meson's attraction is relatively small.

The main contribution to the binding energy comes from the S-wave attractive force. We also plot the effective potential in the first diagram in Fig. 3. V_s and V_d are the effective potential of the S-wave and D-wave interaction after adding the momentum-related terms. V'_s and V'_d are the effective potential of the S-wave and D-wave interaction without the momentum-related terms. We can see a clear difference between V_s and V'_s , which cause an obvious correction to the binding energy when we consider the momentum-related terms.

We first used the computation programme to reproduce the deuteron system successfully. Then we move on to investigate the possibility of X(3872) as the $D\bar{D}^*$ molecular state

with quantum number $I = 0$, $J^{PC} = 1^{++}$. For comparison, we first do not consider the momentum-related terms. Then we add the momentum-related terms and repeat the numerical analysis to investigate its correction to the system.

Considering that the binding energy of X(3872) is tiny, the inclusion of the momentum-related terms may lead to significant corrections to this very loosely bound system.

We collect the numerical results of the binding energy with the variation of the cutoff parameter Λ Table III. E and E' is the eigen-energy of Hamiltonian with and without the momentum-related terms respectively. Besides the total energy, we also list the separate contribution to the energy from the S-wave, D-wave and spin-orbit force components respectively in the fourth, fifth and sixth column. The last column is the mass of X(3872) as a molecular system.

There exists a bound state solution when the cutoff parameter changes from 1.1 \sim 1.3 GeV. The binding energy with the recoil correction is around 0.054 \sim 7.131 MeV and the binding energy without the recoil correction is around 0.276 \sim 9.686 MeV. When the binding energy is 7.131 MeV with $\Lambda = 1.3$ GeV, the recoil correction is 2.555 MeV and the contribution of the spin-orbit force is 0.573 MeV. When the binding energy is 2.361 MeV, the recoil correction is 1.075 MeV and the contribution of the spin-orbit force is 0.213 MeV. When the binding energy decrease to 0.054 with $\Lambda = 1.1$ GeV, the recoil correction reach 0.222 MeV, which is even bigger than the binding energy itself. Now the contribution of the spin-orbit force is 0.038 MeV and almost as big as the D-wave contribution. Clearly the recoil correction decrease the binding energy and renders X(3872) to be an extremely loosely bound molecular states partly.

TABLE III: The bound state solutions of the $D\bar{D}^*$ system with $I^G = 0^+$, $J^{PC} = 1^{++}$ (in unit of MeV) with the cutoff Λ . E and E' is the eigen-energy of the system with and without the momentum-related terms respectively. We also list the separate contribution to the energy from the S-wave, D-wave and spin-orbit components respectively in the fourth, fifth and sixth column. The last column is the mass of X(3872) as a molecular system.

$\Lambda(\text{GeV})$		Eigenvalue				Mass (MeV)
		total	S	D	LS	
1.10	E	-0.054	-4.364	0.052	0.038	3874.846
	E'	-0.276	-4.458	0.017	-	3874.624
1.15	E	-0.884	-10.02	0.128	0.104	3874.016
	E'	-1.449	-10.48	0.031	-	3873.451
1.20	E	-2.361	-17.23	0.245	0.213	3872.539
	E'	-3.436	-18.14	0.046	-	3871.464
1.25	E	-4.469	-24.80	0.401	0.367	3870.431
	E'	-6.203	-26.29	0.059	-	3868.697
1.30	E	-7.131	-32.45	0.609	0.573	3867.769
	E'	-9.686	-34.63	0.076	-	3865.214

B. The $D\bar{D}^*$ system with $I^G = 0^-, J^{PC} = 1^{+-}$

We also calculate the $D\bar{D}^*$ system with $I = 0, J^{PC} = 1^{+-}$. The results with the variation of the cutoff from $1.4 \sim 1.6 \text{ GeV}$ are shown in the Table IV. There might also exist a bound state with odd C parity. Its binding energy is slightly smaller than that of $X(3872)$ with the same cutoff. When the binding energy is 2.386 MeV with $\Lambda = 1.4 \text{ GeV}$, the total recoil correction reaches -0.447 MeV while the contribution of the spin-orbit force is $+0.9 \text{ MeV}$, which is also almost as big as the D-wave contribution. Clearly the recoil correction is favorable to the formation of the molecular state in this channel.

The corresponding effective potential and the exchanged meson's contribution are also shown in the second figure in Fig.3 and Fig.4.

TABLE IV: The bound state solution of the $D\bar{D}^*$ system with $I^G = 0^-, J^{PC} = 1^{+-}$ (in unit of MeV) with Λ . E and E' is the eigenenergy of the system with and without the momentum-related terms respectively. We also list the separate contribution to the energy from the S-wave, D-wave and spin-orbit force components respectively in the fourth, fifth and sixth column. The last column is the mass of the $D\bar{D}^*$ system with $I^G = 0^-, J^{PC} = 1^{+-}$ as a molecular state.

$\Lambda(\text{GeV})$		Eigenvalue				Mass (MeV)
		total	S	D	LS	
1.40	E	-2.386	-10.55	-1.587	0.900	3872.514
	E'	-1.939	-12.30	-2.371	-	3872.961
1.45	E	-7.098	-20.90	-2.863	2.019	3867.802
	E'	-6.298	-24.65	-4.655	-	3868.602
1.50	E	-14.62	-33.88	-4.236	3.635	3860.28
	E'	-13.43	-40.41	-7.513	-	3861.47
1.55	E	-25.20	-49.63	-5.657	5.822	3849.70
	E'	-23.58	-59.87	-10.97	-	3851.32
1.60	E	-39.10	-68.32	-7.074	8.65	3835.80
	E'	-36.95	-83.32	-15.06	-	3837.95

C. $Z_c(3900)$

The newly observed $Z_c(3900)$ was explained as the isovector partner of $X(3872)$ with $J^{PC} = 1^{+-}$ by some theoretical groups [42–44].

We carefully perform the investigation of the $D\bar{D}^*$ system with $I^G = 1^+, J^{PC} = 1^{+-}$. We consider the S-wave and D-wave mixing, the spin orbit force at $O(1/M)$ and all the other possible recoil corrections up to $O(1/M^2)$. The corresponding effective potential and the exchanged meson's contribution are also shown in the fourth diagram in Fig. 3 and Fig. 4. Unfortunately, we are unable to obtain a bound state solution with the pionic coupling $g = 0.59$ which was extracted from the D^* decay width. It seems there probably does not exist a loosely bound isovector molecular state composed of the $D\bar{D}^*$ mesons.

On the other hand, the π meson exchange plays a dominant

role. Considering the uncertainty of g , we try to increase this coupling constant to check the dependence of the results on g . We find when the coupling constant g increases by a factor of 1.6, a bound state appears. The results are listed Table V.

The binding energy of the $J^{PC} = 1^{+-}$ molecule with/without the recoil correction is around $0.037 \sim 15.82 \text{ MeV}$ and $0.322 \sim 18.51 \text{ MeV}$ respectively. When the binding energy is 0.037 MeV , the recoil correction is 0.285 MeV and the contribution of the spin-orbit force is 0.058 MeV . Clearly the recoil corrections are of the same order as the binding energy and unfavorable to the formation of the molecular state.

TABLE V: The $I^G = 1^+, J^{PC} = 1^{+-}$ $D\bar{D}^*$ system with with the enhanced coupling constant g and $\Lambda = 2.0 \text{ GeV}$. The other notations are the same as in Table III.

$g \cdot n$		Eigenvalue				Mass (MeV)
		total	S	D	LS	
$g \cdot 1.6$	E	-0.037	-7.244	0.169	0.058	3874.863
	E'	-0.322	-7.421	0.107	-	3874.578
$g \cdot 1.7$	E	-4.293	-42.32	0.957	0.359	3870.607
	E'	-5.634	-43.21	0.579	-	3869.266
$g \cdot 1.8$	E	-15.82	-93.30	2.007	0.822	3859.08
	E'	-18.51	-95.04	1.146	-	3856.39

D. The $D\bar{D}^*$ system with $I^G = 1^-, J^{PC} = 1^{++}$

We also perform the investigation of the $D\bar{D}^*$ system with $I^G = 1^-, J^{PC} = 1^{++}$. The corresponding effective potential and the exchanged meson's contribution are also shown in the third diagram in Fig. 3 and Fig. 4. There does not exist a bound state solution with the pionic coupling $g = 0.59$. If we increase g by a factor 2.4, there appears a bound state. The numerical results are listed in Table VI.

The binding energy of the possible $J^{PC} = 1^{++}$ state with the recoil correction is around $1.777 \sim 14.49 \text{ MeV}$ while it is around $0.524 \sim 8.67 \text{ MeV}$ without the recoil correction. When the binding energy is 1.777 MeV , the total recoil correction is 1.253 MeV and the contribution of the spin-orbit force alone is -1.903 MeV . The recoil corrections are comparable with the binding energy and very favorable to the formation of the possible loosely bound molecule.

E. The $B\bar{B}^*$ system

The effective potential and meson contributions are shown in Fig. refB-potential and Fig. 6. From Fig. 6, one can see that the π and ρ and ω mesons potentials are comparable.

Let's focus on the the momentum-related correction. From Fig. 5, we can see that the two curves of V_s and V'_s almost overlap. The dominant momentum-related correction comes from the D-wave interaction. In all cases, the momentum-related correction is much smaller than that in the $D\bar{D}^*$ sys-

TABLE VI: The $I^G = 1^-, J^{PC} = 1^{++}$ $D\bar{D}^*$ system with the enhanced coupling constant g and $\Lambda = 2$ GeV. The other notations are the same as in Table III.

$g \cdot n$		Eigenvalue				Mass (MeV)
		total	S	D	LS	
$g \cdot 2.4$	E	-1.777	6.093	-7.074	-1.903	3873.123
	E'	-0.524	6.019	-5.202	-	3874.376
$g \cdot 2.5$	E	-6.518	12.23	-15.67	-4.313	3868.382
	E'	-3.311	12.11	-11.42	-	3871.589
$g \cdot 2.6$	E	-14.49	18.99	-26.35	-7.42	3860.41
	E'	-8.67	18.86	-19.02	-	3866.23

tem, which is expected because the B meson is much heavier than the D meson.

For the $B\bar{B}^*$ system, there exist bound states with the above three kinds of quantum number when varying the cutoff in an appropriate range. We collect the numerical results in Tables VII, VII, IX, X.

The $I^G = 1^+, J^{PC} = 1^{+-}$ bound state corresponds to the candidate of $Z_b(10610)$. The binding energy with the recoil correction is around $0.251 \sim 18.5$ MeV and the binding energy without recoil correction is about $0.348 \sim 19.58$ MeV with the cutoff from $2.1 \sim 2.9$ GeV. When the binding energy is 0.251 MeV, the recoil correction is 0.097 MeV.

For the $I^G = 1^+, J^{PC} = 1^{+-}$ bound state, its binding energy with the recoil correction is around $0.02 \sim 0.446$ MeV and about $0.065 \sim 0.56$ MeV without the recoil correction with the cutoff varies from $4.9 \sim 5.1$ GeV. However, this cutoff may be too larger for a loosely bound system. Its binding energy is much smaller than that of $Z_b(10610)$. When the binding energy is 0.02 MeV, the recoil correction is 0.045 MeV and the contribution of spin-orbit force is 0.04 MeV.

There exist two $I = 0$ bound states which might be the isocalar partners of $Z_b(10610)$. For the $I^G = 0^+, J^{PC} = 1^{++}$ molecule, the binding energy with the recoil correction is about $0.28 \sim 36.87$ MeV when the cutoff varies from $0.7 \sim 1.1$ GeV. When the binding energy is 0.28 MeV, the recoil correction is 0.047 MeV. For the $I^G = 0^-, J^{PC} = 1^{+-}$ molecule, the binding energy with the recoil correction varies from $0.29 \sim 21.09$ MeV with the cutoff around $1.0 \sim 1.2$ GeV.

IV. SUMMARY AND DISCUSSION

In the framework of the one boson exchange model, we have calculated the effective potentials between two heavy mesons from the t - and u -channel π , η , ρ , ω and σ meson exchange. We keep the recoil corrections to the $B\bar{B}^*$ and $D\bar{D}^*$ system up to $O(\frac{1}{M^2})$. We also keep terms related to $\vec{k} = \frac{1}{2}(\vec{p} + \vec{p}')$, which is the sum of the initial and final momentum of the system. Especially, the spin orbit force appears at $O(\frac{1}{M})$, which turns out to be important for the very loosely bound molecular states.

We have carefully investigated the $B\bar{B}^*$ and $D\bar{D}^*$ systems

TABLE VII: The $B\bar{B}^*$ system with $I^G = 1^+, J^{PC} = 1^{+-}$ (in unit of MeV). The other notations are the same as in Table III.

$\Lambda(\text{GeV})$		Eigenvalue				Mass (MeV)
		total	S	D	LS	
2.1	E	-0.251	-6.320	0.079	0.0008	10603.749
	E'	-0.348	-6.337	0.075	-	10603.652
2.3	E	-1.766	-18.76	0.227	0.011	10602.234
	E'	-2.026	-19.11	0.214	-	10601.974
2.5	E	-4.988	-36.17	0.430	0.022	10599.012
	E'	-5.461	-36.21	0.404	-	10598.539
2.7	E	-10.39	-59.52	0.706	0.038	10593.61
	E'	-11.14	-59.56	0.663	-	10592.86
2.9	E	-18.50	-89.71	1.075	0.058	10585.50
	E'	-19.58	-89.74	1.009	-	10584.42

TABLE VIII: The $B\bar{B}^*$ system with $I^G = 1^-, J^{PC} = 1^{++}$ (in unit of MeV). The other notations are the same as in Table III.

$\Lambda(\text{GeV})$		Eigenvalue				Mass (MeV)
		total	S	D	LS	
4.9	E	-0.02	0.772	-0.932	-0.040	10603.98
	E'	-0.065	0.764	-0.895	-	10603.935
4.95	E	-0.089	1.049	-1.252	-0.054	10603.911
	E'	-0.148	1.039	-1.202	-	10603.852
5.0	E	-0.18	1.397	-1.665	-0.072	10603.820
	E'	-0.256	1.384	-1.598	-	10603.744
5.05	E	-0.298	1.809	-2.155	-0.094	10603.702
	E'	-0.392	1.792	-2.068	-	10603.608
5.1	E	-0.446	2.273	-2.710	-0.118	10603.554
	E'	-0.56	2.254	-2.60	-	10603.440

TABLE IX: The $B\bar{B}^*$ system with $I^G = 0^+, J^{PC} = 1^{++}$ (in unit of MeV). The other notations are the same as in Table III.

$\Lambda(\text{GeV})$		Eigenvalue				Mass (MeV)
		total	S	D	LS	
0.7	E	-0.280	-3.174	0.039	0.005	10603.720
	E'	-0.327	-3.178	0.034	-	10603.673
0.8	E	-0.930	-6.631	0.108	0.008	10603.070
	E'	-1.027	-6.615	0.100	-	10602.973
0.9	E	-6.631	-22.31	0.188	0.050	10597.369
	E'	-7.705	-22.45	0.140	-	10596.295
1.0	E	-19.08	-44.46	0.034	0.206	10584.920
	E'	-20.42	-45.08	0.663	-	10583.58
1.1	E	-36.87	-67.91	0.403	0.590	10567.13
	E'	-39.87	-69.45	-0.158	-	10643.87

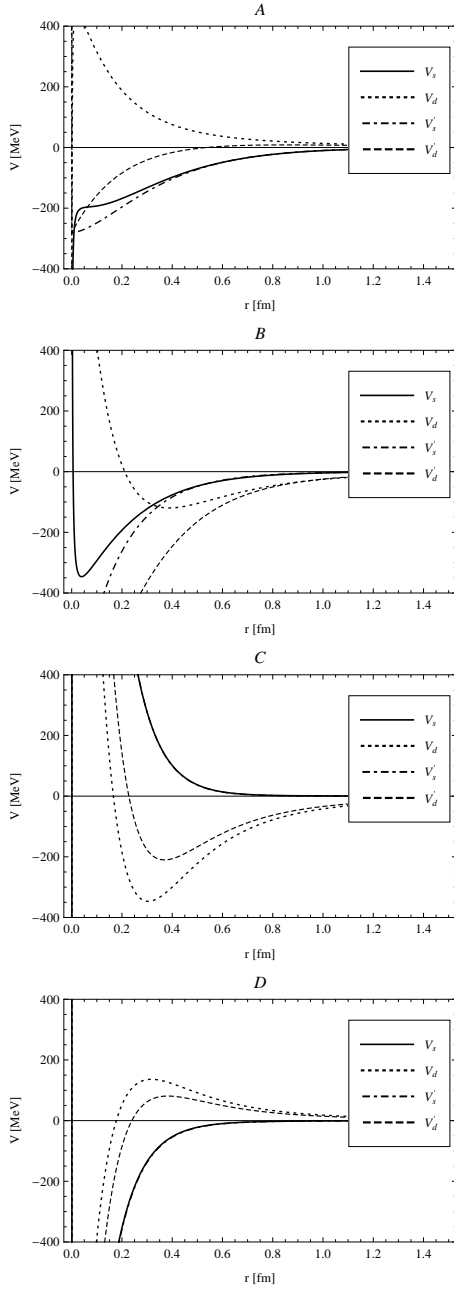


FIG. 3: The effective potential of the $D\bar{D}^*$ system. Labels A,B,C,D correspond to the four cases $I = 0, J^{PC} = 1^{++}$; $I = 0, J^{PC} = 1^{+-}$; $I = 1, J^{PC} = 1^{++}$; $I = 1, J^{PC} = 1^{+-}$ respectively from top to bottom. V_s and V_d are the effective potential of the S-wave and D-wave interaction with the momentum-related terms while V'_s and V'_d are the S-wave and D-wave effective potential without the momentum-related terms.

with four kinds of quantum number: $I = 0, J^{PC} = 1^{++}$; $I = 0, J^{PC} = 1^{+-}$; $I = 1, J^{PC} = 1^{++}$; $I = 1, J^{PC} = 1^{+-}$.

After solving the Schrödinger equation by the variation method, we notice that there exist two isoscalar $D\bar{D}^*$ molecular states with $J^{PC} = 1^{++}$ and $J^{PC} = 1^{+-}$ with or without the momentum-related corrections. The first C-parity even 1^{++}

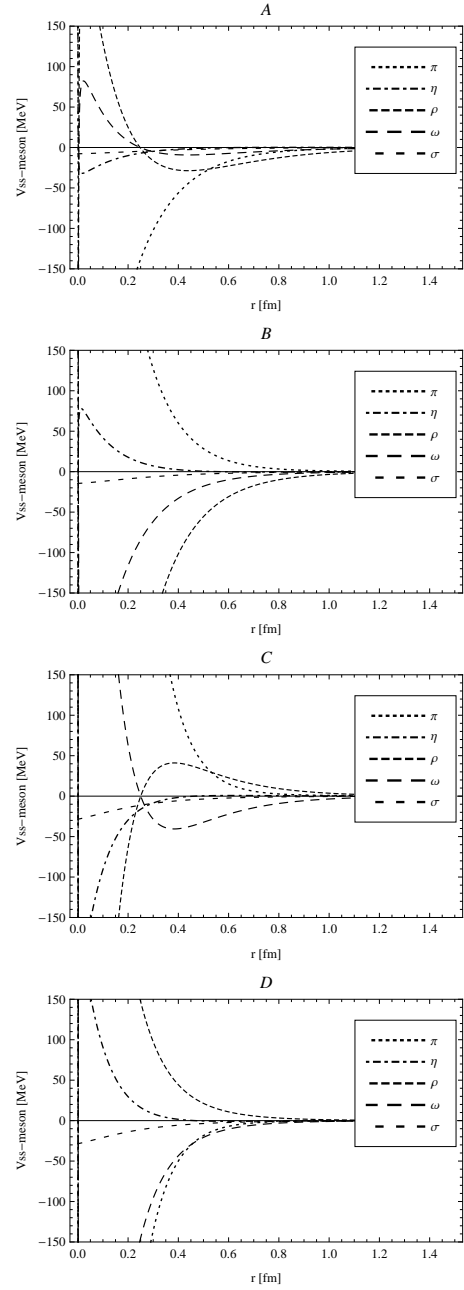


FIG. 4: The effective potential from the different meson exchange in the $D\bar{D}^*$ system. Labels A,B,C,D are the same as in Fig. 3.

state corresponds to $X(3872)$. In contrast, there exist loosely bound states in three channels for the $B\bar{B}^*$ system with the cutoff in a reasonable range.

Our numerical results show that the momentum-related corrections are unfavorable to the formation of the loosely bound molecular states in the $I = 0, J^{PC} = 1^{++}$ and $I = 1, J^{PC} = 1^{+-}$ channels in the $D\bar{D}^*$ system. Especially the recoil corrections are quite large. For example, the recoil correction may be larger than the binding energy of $X(3872)$, which may partly force $X(3872)$ to become a very shallow bound state. As ex-

TABLE X: The $B\bar{B}^*$ system with $I^G = 0^-$, $J^{PC} = 1^{+-}$ (in unit of MeV). The other notations are the same as in Table III.

$\Lambda(\text{GeV})$		Eigenvalue				Mass (MeV)
		total	S	D	LS	
1.0	E	-0.290	-0.042	-0.568	0.023	10603.710
	E'	-0.290	-0.049	-0.584	-	10603.710
1.05	E	-1.838	-0.502	-1.832	0.132	10602.162
	E'	-1.841	-0.548	-1.936	-	10602.159
1.1	E	-5.388	-1.992	-3.794	0.409	10598.612
	E'	-5.439	-2.145	-4.135	-	10598.561
1.15	E	-11.60	-5.079	-6.447	0.939	10592.40
	E'	-11.81	-5.451	-7.256	-	10592.19
1.2	E	-21.02	-10.24	9.779	1.798	10582.98
	E'	-21.59	-10.99	-11.37	-	10582.41

pected, the recoil correction in the $D\bar{D}^*$ system is much larger than that in the $B\bar{B}^*$ system.

However, we are unable to find a bound state for the $D\bar{D}^*$ system with $I = 1$, $J^{PC} = 1^{++}$ and $I = 1$, $J^{PC} = 1^{+-}$ with the pionic coupling $g = 0.59$ which was extracted from the D^* decay width and plays a dominant role in the effective potential, although we have systematically included the S-D wave mixing effect, the spin orbit force and all the other recoil corrections up to $O(\frac{1}{M^2})$. A loosely bound state appears if we increase g manually by a factor of 1.6 \sim 1.8 after the inclusion of the recoil corrections.

It seems that it's not so easy to accommodate the newly observed charged resonance $Z_c(3900)$ as the candidate of the isovector molecular state of $D\bar{D}^*$. The present investigation shows that the recoil corrections may diminish the binding energy by one to several MeV and are unfavorable to the formation of loosely bound molecular states in this channel. Experimentally the mass $Z_c(3900)$ seems above the $D\bar{D}^*$ threshold. Our analysis shows that there does exist attraction in this channel. One may wonder whether $Z_c(3900)$ is a candidate of the molecular-type resonance instead of a $D\bar{D}^*$ bound state.

On the other hand, we should also inspect the framework of the one boson exchange model. One obvious uncertainty arises from the cutoff parameter, which is commonly used to suppress the high momentum contribution. Moreover, in the derivation of the effective potential, we make Fourier transformation to the effective potential in the momentum space to derive the potential in the coordinate space. In case of the $D\bar{D}^*$ system, the mass splitting between D and \bar{D}^* is larger than the pion mass. Hence the integral contains an imaginary part. The commonly used approach is to take the principal value of this integral and omit the imaginary part in order to ensure the effective potential and Hamiltonian to be real. The resulting potential is oscillating. The reliability of such a formalism deserves further investigation.

In short, the XYZ states provide a unique platform to study the complicated low energy strong dynamics. The charmonium (or Upsilon) spectrum above the open charm (or bottom) threshold and those charmonium-like XYZ states as non-

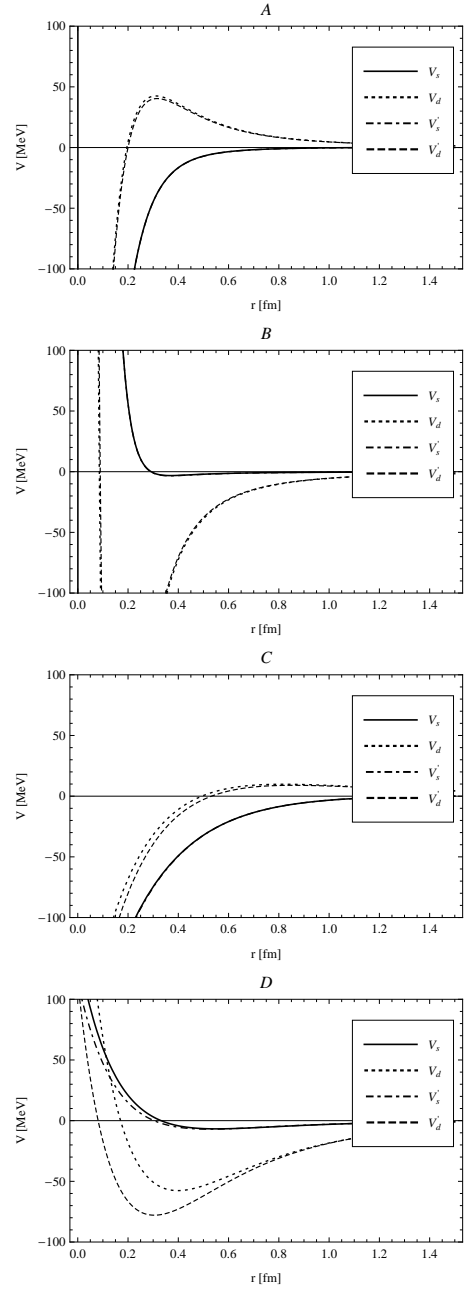


FIG. 5: The effective potential of the $B\bar{B}^*$ system. Notations are the same as in Fig. 3.

conventional candidates are particularly interesting. In order to interpret their underlying structures, we need also investigate their decay pattern and production mechanisms.

V. ACKNOWLEDGEMENT

We thank Li-Ping Sun, Zhi-Feng Sun and Li Ning for useful discussions. This project is supported by the National Natural Science Foundation of China under Grant No. 11261130311.

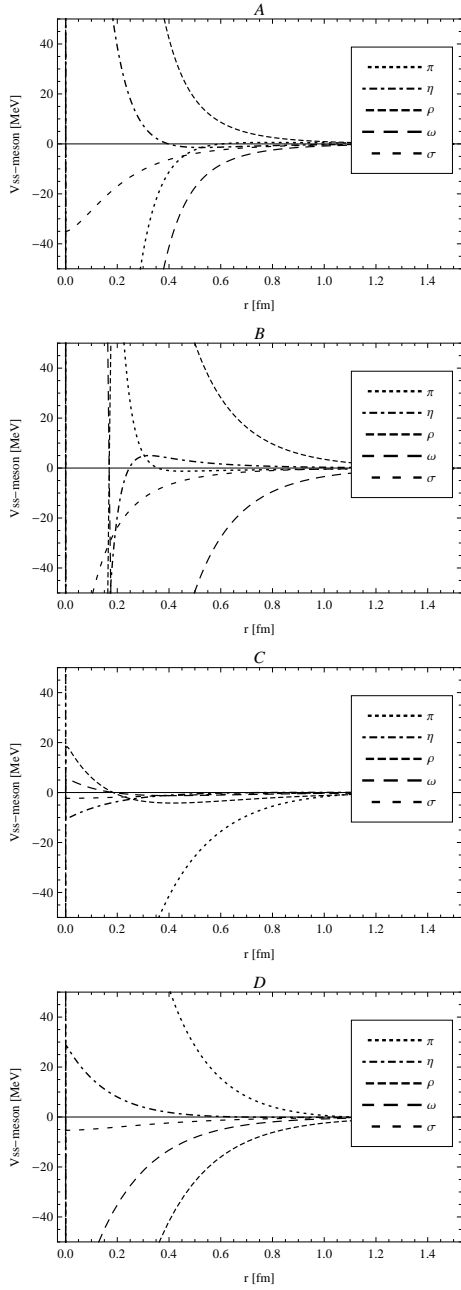


FIG. 6: The effective potential from the different meson exchange in the $B\bar{B}^*$ system. Labels A,B,C,D are the same as in Fig. 3.

VI. APPENDIX

We collect the expressions of the functions used in the previous sections in the appendix.

$$Y(\tilde{m}_\alpha r) = \frac{\exp(\tilde{m}_\alpha r)}{\tilde{m}_\alpha r} \quad (50)$$

$$Z(\tilde{m}_\alpha r) = \left(1 + \frac{3}{\tilde{m}_\alpha r} + \frac{3}{(\tilde{m}_\alpha r)^2}\right) Y(\tilde{m}_\alpha r) \quad (51)$$

$$Z_1(\tilde{m}_\alpha r) = \left(\frac{1}{\tilde{m}_\alpha r} + \frac{1}{(\tilde{m}_\alpha r)^2}\right) Y(\tilde{m}_\alpha r) \quad (52)$$

$$Z'(\tilde{m}_\alpha r) = \frac{\sin(\tilde{m}_\alpha r)}{\tilde{m}_\alpha r} - \frac{3}{\tilde{m}_\alpha r} \frac{\sin(\tilde{m}_\alpha r)}{\tilde{m}_\alpha r} + \frac{1}{(\tilde{m}_\alpha r)^2} \frac{\cos(\tilde{m}_\alpha r)}{\tilde{m}_\alpha r}. \quad (53)$$

$$Z'_1(\tilde{m}_\alpha r) = \frac{1}{\tilde{m}_\alpha r} \frac{\sin(\tilde{m}_\alpha r)}{\tilde{m}_\alpha r} + \frac{1}{(\tilde{m}_\alpha r)^2} \frac{\cos(\tilde{m}_\alpha r)}{\tilde{m}_\alpha r} \quad (54)$$

where for the $D\bar{D}^*$ system

$$\tilde{m}_\pi^2 = (m_D^* - m_D)^2 - m_\pi^2, \quad (55)$$

$$\tilde{m}_{\sigma,\rho,\omega,\eta}^2 = m_{\sigma,\rho,\omega,\eta}^2 - (m_D^* - m_D)^2. \quad (56)$$

while for the $B\bar{B}^*$ system

$$\tilde{m}_{\pi,\sigma,\rho,\omega,\eta}^2 = m_{\pi,\sigma,\rho,\omega,\eta}^2 - (m_B^* - m_B)^2. \quad (57)$$

$$\begin{aligned} \mathcal{F}_{1t\alpha} &= \mathcal{F}\left\{\left(\frac{\Lambda^2 - m_\alpha^2}{\Lambda^2 + \vec{q}^2}\right) \frac{1}{\vec{q}^2 + m_\alpha^2}\right\} \\ &= m_\alpha Y(m_\alpha r) - \Lambda Y(\Lambda r) - (\Lambda^2 - m_\alpha^2) \frac{e^{-\Lambda r}}{2\Lambda} \end{aligned} \quad (58)$$

$$\begin{aligned} \mathcal{F}_{1u\alpha} &= \mathcal{F}\left\{\left(\frac{\Lambda^2 - m_\alpha^2}{\tilde{\Lambda}^2 + \vec{q}^2}\right) \frac{1}{\vec{q}^2 + \tilde{m}_\alpha^2}\right\} \\ &= \tilde{m}_\alpha Y(\tilde{m}_\alpha r) - \tilde{\Lambda} Y(\tilde{\Lambda} r) - (\Lambda^2 - m_\alpha^2) \frac{e^{-\tilde{\Lambda} r}}{2\tilde{\Lambda}} \end{aligned} \quad (59)$$

$$\begin{aligned} \mathcal{F}_{2t\alpha} &= \mathcal{F}\left\{\left(\frac{\Lambda^2 - m_\alpha^2}{\Lambda^2 + \vec{q}^2}\right) \frac{\vec{q}^2}{\vec{q}^2 + m_\alpha^2}\right\} \\ &= m_\alpha^2 [\Lambda Y(\Lambda r) - m_\alpha Y(m_\alpha r)] \\ &\quad + (\Lambda^2 - m_\alpha^2) \Lambda \frac{e^{-\Lambda r}}{2} \end{aligned} \quad (60)$$

$$\begin{aligned} \mathcal{F}_{2u\alpha} &= \mathcal{F}\left\{\left(\frac{\Lambda^2 - m_\alpha^2}{\tilde{\Lambda}^2 + \vec{q}^2}\right) \frac{\vec{q}^2}{\vec{q}^2 + \tilde{m}_\alpha^2}\right\} \\ &= \tilde{m}_\alpha^2 [\tilde{\Lambda} Y(\tilde{\Lambda} r) - \tilde{m}_\alpha Y(\tilde{m}_\alpha r)] \\ &\quad + (\Lambda^2 - m_\alpha^2) \tilde{\Lambda} \frac{e^{-\tilde{\Lambda} r}}{2} \end{aligned} \quad (61)$$

$$\begin{aligned} \mathcal{F}_{3t\alpha} &= \mathcal{F}\left\{\left(\frac{\Lambda^2 - m_\alpha^2}{\Lambda^2 + \vec{q}^2}\right) \frac{(\vec{\sigma}_1 \cdot \vec{q})(\vec{\sigma}_2 \cdot \vec{q})}{\vec{p}^2 + m_\alpha^2}\right\} \\ &= \frac{1}{3} \vec{\sigma}_1 \cdot \vec{\sigma}_2 [m_\alpha^2 \Lambda Y(\Lambda r) - m_\alpha^3 Y(m_\alpha r) \\ &\quad + (\Lambda^2 - m_\alpha^2) \Lambda \frac{e^{-\Lambda r}}{2}] \\ &\quad + \frac{1}{3} S_{12} [-m_\alpha^3 Z(m_\alpha r) + \Lambda^3 Z(\Lambda r) \\ &\quad + (\Lambda^2 - m_\alpha^2)(1 + \Lambda r) \frac{\Lambda}{2} Y(\Lambda r)] \\ &= (\vec{\sigma}_1 \cdot \vec{\sigma}_2) \mathcal{F}_{3t1} + S_{12} \mathcal{F}_{3t2} \end{aligned} \quad (62)$$

$$\begin{aligned}
\mathcal{F}_{3u\alpha} &= \mathcal{F}\left\{\left(\frac{\Lambda^2 - m_\alpha^2}{\tilde{\Lambda}^2 + \vec{q}^2}\right) \frac{(\vec{\sigma}_1 \cdot \vec{q})(\vec{\sigma}_2 \cdot \vec{q})}{\vec{q}^2 + \tilde{m}_\alpha^2}\right\} \\
&= \frac{1}{3} \vec{\sigma}_1 \cdot \vec{\sigma}_2 [\tilde{m}_\alpha^2 \tilde{\Lambda} Y(\tilde{\Lambda} r) - \tilde{m}_\alpha^3 Y(\tilde{m}_\alpha r) \\
&\quad + (\Lambda^2 - m_\alpha^2) \tilde{\Lambda} \frac{e^{-\tilde{\Lambda} r}}{2}] \\
&\quad + \frac{1}{3} S_{12} [-\tilde{m}_\alpha^3 Z(\tilde{m}_\alpha r) + \tilde{\Lambda}^3 Z(\tilde{\Lambda} r) \\
&\quad + (\Lambda^2 - m_\alpha^2)(1 + \tilde{\Lambda} r) \frac{\tilde{\Lambda}}{2} Y(\tilde{\Lambda} r)] \\
&= (\vec{\sigma}_1 \cdot \vec{\sigma}_2) \mathcal{F}_{3u1\alpha} + S_{12} \mathcal{F}_{3u2\alpha} \tag{63}
\end{aligned}$$

$$\begin{aligned}
\mathcal{F}'_{3u\alpha} &= \mathcal{F}\left\{\left(\frac{\Lambda^2 - m_\alpha^2}{\tilde{\Lambda}^2 + \vec{q}^2}\right) \frac{(\vec{\sigma}_1 \cdot \vec{q})(\vec{\sigma}_2 \cdot \vec{q})}{\vec{p}^2 - \tilde{m}_\alpha^2}\right\} \\
&= \frac{1}{3} \vec{\sigma}_1 \cdot \vec{\sigma}_2 [-\tilde{m}_\alpha^2 \tilde{\Lambda} Y(\tilde{\Lambda} r) - \tilde{m}_\alpha^3 \frac{\cos(\tilde{m}_\alpha r)}{\tilde{m}_\alpha r} \\
&\quad + (\Lambda^2 - m_\alpha^2) \tilde{\Lambda} \frac{e^{-\tilde{\Lambda} r}}{2}] \\
&\quad + \frac{1}{3} S_{12} [\tilde{m}_\alpha^3 Z'(\tilde{m}_\alpha r) + \tilde{\Lambda}^3 Z(\tilde{\Lambda} r) \\
&\quad + (\Lambda^2 - m_\alpha^2)(1 + \tilde{\Lambda} r) \frac{\tilde{\Lambda}}{2} Y(\tilde{\Lambda} r)] \\
&= (\vec{\sigma}_1 \cdot \vec{\sigma}_2) \mathcal{F}'_{3u1\alpha} + S_{12} \mathcal{F}'_{3u2\alpha} \tag{64}
\end{aligned}$$

$$\begin{aligned}
\mathcal{F}_{4t\alpha} &= \mathcal{F}\left\{\left(\frac{\Lambda^2 - m_\alpha^2}{\Lambda^2 + \vec{q}^2}\right) \frac{\vec{k}^2}{\vec{q}^2 + m_\alpha^2}\right\} \\
&= \frac{m_\alpha^3}{4} Y(m_\alpha r) - \frac{\Lambda^3}{4} Y(\Lambda r) \\
&\quad - \frac{\Lambda^2 - m_\alpha^2}{4} \left(\frac{\Lambda r}{2} - 1\right) \frac{e^{-\Lambda r}}{r} \\
&\quad - \frac{1}{2} \{\nabla^2, m_\alpha Y(m_\alpha r) - \Lambda Y(\Lambda r) - \frac{\Lambda^2 - m_\alpha^2}{2} \frac{e^{-\Lambda r}}{\Lambda}\} \\
&= \mathcal{F}_{4t1\alpha} + \{-\frac{1}{2} \nabla^2, \mathcal{F}_{4t2\alpha}\} \tag{65}
\end{aligned}$$

$$\begin{aligned}
\mathcal{F}_{4u\alpha} &= \mathcal{F}\left\{\left(\frac{\Lambda^2 - \tilde{m}_\alpha^2}{\tilde{\Lambda}^2 + \vec{q}^2}\right) \frac{\vec{k}^2}{\vec{q}^2 + \tilde{m}_\alpha^2}\right\} \\
&= \frac{\tilde{m}_\alpha^3}{4} Y(\tilde{m}_\alpha r) - \frac{\tilde{\Lambda}^3}{4} Y(\tilde{\Lambda} r) \\
&\quad - \frac{\Lambda^2 - m_\alpha^2}{4} \left(\frac{\tilde{\Lambda} r}{2} - 1\right) \frac{e^{-\tilde{\Lambda} r}}{r} \\
&\quad - \frac{1}{2} \{\nabla^2, \tilde{m}_\alpha Y(\tilde{m}_\alpha r) - \tilde{\Lambda} Y(\tilde{\Lambda} r) - \frac{\Lambda^2 - m_\alpha^2}{2} \frac{e^{-\tilde{\Lambda} r}}{\tilde{\Lambda}}\} \\
&= \mathcal{F}_{4u1\alpha} + \{-\frac{1}{2} \nabla^2, \mathcal{F}_{4u2\alpha}\} \tag{66}
\end{aligned}$$

$$\begin{aligned}
\mathcal{F}_{5t\alpha} &= \mathcal{F}\left\{i\left(\frac{\Lambda^2 - m_\alpha^2}{\Lambda^2 + \vec{q}^2}\right) \frac{\vec{S} \cdot (\vec{q} \times \vec{k})}{\vec{q}^2 + m_\alpha^2}\right\} \\
&= \vec{S} \cdot \vec{L} [-m_\alpha^3 Z_1(m_\alpha r) + \Lambda^3 Z_1(\Lambda r) \\
&\quad + (\Lambda^2 - m_\alpha^2) \frac{e^{-\Lambda r}}{2r}] \\
&= \vec{S} \cdot \vec{L} \mathcal{F}_{5t0\alpha} \tag{67}
\end{aligned}$$

$$\begin{aligned}
\mathcal{F}_{5u\alpha} &= \mathcal{F}\left\{i\left(\frac{\Lambda^2 - m_\alpha^2}{\tilde{\Lambda}^2 + \vec{q}^2}\right) \frac{\vec{S} \cdot (\vec{q} \times \vec{k})}{\vec{q}^2 + \tilde{m}_\alpha^2}\right\} \\
&= \vec{S} \cdot \vec{L} [-\tilde{m}_\alpha^3 Z_1(\tilde{m}_\alpha r) + \tilde{\Lambda}^3 Z_1(\tilde{\Lambda} r) \\
&\quad + (\Lambda^2 - m_\alpha^2) \frac{e^{-\tilde{\Lambda} r}}{2r}] \\
&= \vec{S} \cdot \vec{L} \mathcal{F}_{5u0\alpha} \tag{68}
\end{aligned}$$

$$\begin{aligned}
\mathcal{F}'_{5u\alpha} &= \mathcal{F}\left\{i\left(\frac{\Lambda^2 - m_\alpha^2}{\tilde{\Lambda}^2 + \vec{q}^2}\right) \frac{\vec{S} \cdot (\vec{q} \times \vec{k})}{\vec{q}^2 + \tilde{m}_\alpha^2}\right\} \\
&= \vec{S} \cdot \vec{L} [-\tilde{m}_\alpha^3 Z'_1(\tilde{m}_\alpha r) + \tilde{\Lambda}^3 Z_1(\tilde{\Lambda} r) \\
&\quad + (\Lambda^2 - m_\alpha^2) \frac{e^{-\tilde{\Lambda} r}}{2r}] \\
&= \vec{S} \cdot \vec{L} \mathcal{F}'_{5u0\alpha} \tag{69}
\end{aligned}$$

$$\begin{aligned}
\mathcal{F}_{6u\alpha} &= \mathcal{F}\left\{\left(\frac{\Lambda^2 - m_\alpha^2}{\tilde{\Lambda}^2 + \vec{q}^2}\right) \frac{(\vec{\sigma}_1 \cdot \vec{k})(\vec{\sigma}_2 \cdot \vec{k})}{\vec{p}^2 + \tilde{m}_\alpha^2}\right\} \\
&= -\frac{\vec{\sigma}_1 \cdot \vec{\sigma}_2}{4} [\tilde{m}_\alpha^3 Y(\tilde{m}_\alpha r) - (\tilde{\Lambda})^3 Y(\tilde{\Lambda} r) \\
&\quad - (\Lambda^2 - m_\alpha^2) \tilde{\Lambda} \frac{e^{-\tilde{\Lambda} r}}{2}] \\
&\quad + \frac{1}{3} (S_{12} + \vec{\sigma}_1 \cdot \vec{\sigma}_2) [(1 + \frac{3}{\tilde{m}_\alpha r}) \tilde{m}_\alpha^2 Y(\tilde{\Lambda} r) \\
&\quad - (1 + \frac{3}{\tilde{\Lambda} r}) (\tilde{\Lambda})^2 Y(\tilde{\Lambda} r) \\
&\quad - (\Lambda^2 - m_\alpha^2) (\tilde{\Lambda} + \frac{2}{r}) \frac{e^{-\tilde{\Lambda} r}}{2\tilde{\Lambda}}] \nabla \\
&\quad - \frac{1}{3} (S_{12} + \vec{\sigma}_1 \cdot \vec{\sigma}_2) [\tilde{m}_\alpha Y(\tilde{m}_\alpha r) - \tilde{\Lambda} Y(\tilde{\Lambda} r) \\
&\quad - (\Lambda^2 - m_\alpha^2) \frac{e^{-\tilde{\Lambda} r}}{2\tilde{\Lambda}}] \nabla^2 \\
&= -\frac{\vec{\sigma}_1 \cdot \vec{\sigma}_2}{4} \mathcal{F}_{6u1\alpha} + \frac{1}{3} (S_{12} + \vec{\sigma}_1 \cdot \vec{\sigma}_2) \mathcal{F}_{6u2\alpha} \\
&\quad - \frac{1}{3} (S_{12} + \vec{\sigma}_1 \cdot \vec{\sigma}_2) \mathcal{F}_{6u3\alpha} \tag{70}
\end{aligned}$$

$$\begin{aligned}
\mathcal{F}'_{6u\alpha} &= \mathcal{F}\left\{\left(\frac{\Lambda^2 - m_\alpha^2}{\tilde{\Lambda}^2 + \vec{q}^2}\right) \frac{(\vec{\sigma}_1 \cdot \vec{k})(\vec{\sigma}_2 \cdot \vec{k})}{\vec{p}^2 - \tilde{m}_\alpha^2}\right\} \\
&= -\frac{\vec{\sigma}_1 \cdot \vec{\sigma}_2}{4} \left[\tilde{m}_\alpha^3 \frac{\cos(\tilde{m}_\alpha r)}{\tilde{m}_\alpha r} - (\tilde{\Lambda})^3 Y(\tilde{\Lambda} r) \right. \\
&\quad \left. - (\Lambda^2 - m_\alpha^2) \tilde{\Lambda} \frac{e^{-\tilde{\Lambda} r}}{2} \right] \\
&\quad + \frac{1}{3} (S_{12} + \vec{\sigma}_1 \cdot \vec{\sigma}_2) \left[\left(\frac{\sin(\tilde{m}_\alpha r)}{\tilde{m}_\alpha r} + \frac{3}{\tilde{m}_\alpha r} \frac{\cos(\tilde{m}_\alpha r)}{\tilde{m}_\alpha r} \right) \tilde{m}_\alpha^2 \right. \\
&\quad \left. - \left(1 + \frac{3}{\tilde{\Lambda} r} \right) (\tilde{\Lambda})^2 Y(\tilde{\Lambda} r) - (\Lambda^2 - m_\alpha^2) \left(\tilde{\Lambda} + \frac{2}{r} \right) \frac{e^{-\tilde{\Lambda} r}}{2\tilde{\Lambda}} \right] \nabla \\
&\quad - \frac{1}{3} (S_{12} + \vec{\sigma}_1 \cdot \vec{\sigma}_2) \left[\tilde{m}_\alpha \frac{\cos(\tilde{m}_\alpha r)}{\tilde{m}_\alpha r} - \tilde{\Lambda} Y(\tilde{\Lambda} r) \right. \\
&\quad \left. - (\Lambda^2 - m_\alpha^2) \frac{e^{-\tilde{\Lambda} r}}{2\tilde{\Lambda}} \right] \nabla^2 \\
&= -\frac{\vec{\sigma}_1 \cdot \vec{\sigma}_2}{4} \mathcal{F}'_{6u1\alpha} + \frac{1}{3} (S_{12} + \vec{\sigma}_1 \cdot \vec{\sigma}_2) \mathcal{F}'_{6u2\alpha} \\
&\quad - \frac{1}{3} (S_{12} + \vec{\sigma}_1 \cdot \vec{\sigma}_2) \mathcal{F}'_{6u3\alpha} \tag{71}
\end{aligned}$$

-
- [1] R. Mizuk *et al.*, Belle Collaboration, Phys. Rev. **D78**, 072004 (2008).
- [2] S.K. Choi *et al.*, Belle Collaboration, Phys. Rev. Lett. **100**, 142001 (2008).
- [3] K. Chilikin *et al.*, Belle Collaboration, Phys. Rev. **D88**, 074026 (2013).
- [4] M. Ablikim *et al.*, BESIII Collaboration, Phys. Rev. Lett. **110**, 252001 (2013).
- [5] F.E. Close and P.R. Page, Phys. Lett. **B578**, 119 (2004).
- [6] M.B. Voloshin, Phys. Lett. **B579**, 316 (2004).
- [7] C.Y. Wong, Phys. Rev. **C69**, 055202 (2004).
- [8] E.S. Swanson, Phys. Lett. **B588**, 189 (2004).
- [9] N.A. Törnqvist, Phys. Lett. **B590**, 209 (2004).
- [10] Y.-R. Liu, M. Oka, M. Takizawa, X. Liu, W.-Z. Deng and S.-L. Zhu, Phys. Rev. **D82**, 014011 (2010).
- [11] B.-A. Li, Phys. Lett. **B605**, 306 (2005).
- [12] H. Hogaasen, J.M. Richard and P. Sorba, Phys. Rev. **D73**, 054013 (2006).
- [13] D. Ebert, R.N. Faustov and V.O. Galkin, Phys. Lett. **B634**, 214 (2006).
- [14] N. Barnea, J. Vijande and A. Valcarce, Phys. Rev. **D73**, 054004 (2006).
- [15] Y. Cui, X.L. Chen, W.Z. Deng and S.L. Zhu, High Energy Phys. Nucl. Phys. **31**, 7 (2007).
- [16] R.D. Matheus, S. Narison, M. Nielsen and J.M. Richard, Phys. Rev. **D75**, 014005 (2007).
- [17] T.W. Chiu and T.H. Hsieh, Phys. Lett. **B646**, 95 (2007).
- [18] D. Gamermann and E. Oset, Eur. Phys. J. **A33**, 119 (2007).
- [19] S.K. Choi *et al.*, Belle Collaboration, Phys. Rev. Lett. **91**, 262001 (2003).
- [20] M.T. AlFiky, F. Gabbiani and A.A. Petrov, Phys. Lett. **B640**, 238 (2006).
- [21] S. Fleming, M. Kusunoki, T. Mehen, and U. van Kolck, Phys. Rev. **D76**, 034006 (2007).
- [22] E. Braaten, Meng Lu and J. Lee, Phys. Rev. **D76**, 054010 (2007).
- [23] C. Hanhart, Y.S. Kalashnikova, A.E. Kudryavtsev, and A.V. Nefediev, Phys. Rev. **D76**, 034007 (2007).
- [24] M.B. Voloshin, Phys. Rev. **D76**, 014007 (2007).
- [25] P. Colangelo, F. De Fazio and S. Nicotri, Phys. Lett. **B650**, 166 (2007).
- [26] M. Suzuki, Phys. Rev. **D72**, 114013 (2005).
- [27] S.L. Zhu, Int. J. Mod. Phys. **E17**, 283 (2008).
- [28] I. Adachi *et al.*, Belle Collaboration, arXiv:1105.4583 [hep-ex]
- [29] Y.-R. Liu, X. Liu, W.-Z. Deng and S.-L. Zhu, Eur. Phys. J. **C56**, 63 (2008).
- [30] X. Liu, L.-Z. Gang, Y.-R. Liu, and S.-L. Zhu, Eur. Phys. J. **C61**, 411 (2009).
- [31] A.E. Bondar, A. Garmash, A.I. Milstein, R. Mizuk and M.B. Voloshin, arXiv:1105.4437 [hep-ph]
- [32] D.-Y. Chen, X. Liu and S.-L. Zhu, Phys. Rev. **D84**, 074016 (2011).
- [33] Z.-F. Sun, J. He, X. Liu, Z.-G. Luo and S.-L. Zhu, Phys. Rev. **D84**, 054002 (2011).
- [34] T. Xiao, S. Dobbs, A. Tomaradze and Kamal K. Seth, Phys. Lett. **B727**, 266 (2013).
- [35] Z.-Q. Liu *et al.*, Belle Collaboration, Phys. Rev. Lett. **110**, 252002 (2013).
- [36] N. Li and S.-L. Zhu, Phys. Rev. **D86**, 074022 (2012).
- [37] S. Ahmed *et al.*, CLEO Collaboration, Phys. Rev. Lett. **87**, 251801 (2001).
- [38] C. Isola, M. Ladisa, G. Nardulli and P. Santorelli, Phys. Rev. **D68**, 114001 (2003).
- [39] C. Isola, M. Ladisa, G. Nardulli and P. Santorelli, Phys. Rept. **164**, 217 (1988).
- [40] A. F. Falk and M. E. Luke, Phys. Lett. **B292**, 119 (1992).
- [41] K. Nakamura, *et al.*, Particle Data Group, J. Phys. **G37**, 075021 (2010).

- [42] Q. Wang, C. Hanhart and Q. Zhao, arXiv:1303.6355 [hep-ph]
- [43] Z.-G. Wang, T. Huang, arXiv:1312.7489 [hep-ph]
- [44] F. Aceti, M. Bayar, E. Oset, A. Martinez Torres, K. P. Khemchandani, F. S. Navarra and M. Nielsen, arXiv:1401.8216 [hep-ph]